

THERMODYNAMIC ASSESSMENT OF THE Mg-Pb and Mg-Bi SYSTEMS USING SUBSTITUTIONAL SOLUTION AND ASSOCIATE MODELS FOR THE LIQUID PHASE

F. Zhang^a, Y. Tang^a, B. Hu^a, S. Liu^{a*}, Y. Du^a, Y. Zhang^b

^a State Key Laboratory of Powder Metallurgy, Central South University, Changsha, PR China

^b PhosphorTech Inc 3645 Kennesaw N Industrial Par Kennesaw, GA, United States

(Received 24 August 2013; accepted 15 April 2014)

Abstract

By means of CALPHAD approach, thermodynamic assessments of the Mg-Pb and Mg-Bi systems were carried out based on the available experimental data including thermodynamic properties and phase equilibrium data. The liquid phase was described with both the substitutional solution model and the associate model, and two sets of self-consistent thermodynamic parameters for the Mg-Pb and Mg-Bi systems were obtained, respectively. It was found that the associate model can account for the experimental data more satisfactorily than the substitutional solution one, especially for the liquid phase with the short-range order behavior.

Keywords: associativity; substitution; phases; thermodynamics

1. Introduction

Mg-based alloys have attracted world-wide attention due to their low density, good machinability, excellent specific strength, and high recycling potential [1]. The Mg alloys with Pb or Bi addition can increase the creep-resistant [2] and tensile strength [3]. These alloys have been widely used in electronic consumer products and transportation industry due to the increasingly urgent demand for weight reduction during the past decades. In order to predict the phase type, phase fraction or reaction during the materials preparation process for development and design of Mg-based alloys containing Pb and Bi, the information of phase equilibria and thermodynamics of Mg-Pb and Mg-Bi binary systems will be very useful. Besides, an accurate thermodynamic description of the Mg-Pb and Mg-Bi system is necessary in order to provide a reliable basis for thermodynamic extrapolations and calculations in related ternary and higher order systems.

Several groups [4-9] reported that the liquid of the Mg-Pb and Mg-Bi systems show the short-range order behavior. Due to the anomalies of the thermodynamic properties, it is difficult to describe the liquid phase by using the regular model. Therefore, several groups of authors [9-13] described the liquid phase of these two systems using the associate model [14, 15], the modified quasichemical model [16] and two-

sublattice model. However, there still exist some problems for the present thermodynamic modeling of the Mg-Pb and Mg-Bi systems. Firstly, the calculated phase diagram of the Mg-Bi system from previous parameters [10, 12, 13] show a large deviation from the experimental data in the composition range from 40 to 60 at.% Bi. Secondly, it is not reasonable to use the polynomial $a+bT+cT\ln T$ by Chang-seok et al. [10] and Niu et al. [13] when there is no sufficient experimental data to describe the Gibbs energy of compound phase (α -Mg₃Bi₂ and β -Mg₃Bi₂). Besides, the thermodynamic parameters from the latest version of the two systems in the literature [11, 12] cannot be directly utilized in our multi-component Mg alloy thermodynamic database [17] due to the model incompatibility. Therefore, thermodynamic reassessments of these two systems are necessary.

The present work is devoted to performing a full thermodynamic modeling of the Mg-Bi and Mg-Pb systems by using both substitutional solution model and the associate model to describe the liquid phase via CALPHAD approach.

2. Literature review

The available literature data of the Mg-Bi and Mg-Pb systems, including phase diagram and thermochemical properties data, were critically reviewed in the present work and summarized in Table 1.

* Corresponding author: shhliu@csu.edu.cn

2.1 The Mg-Pb system

The experimental phase diagram and thermodynamic data of the Mg-Pb system in the literature have been evaluated by Nayeb-Hashemi and Clark [18]. After that, only a few experimental data [19] have been reported. By means of thermal

analysis (TA) and differential thermal analysis (DTA), the liquidus of the Mg-Pb system were determined by several groups [20-27]. However, the experimental data around 50-60 at.% Pb from Grube [20] showed a large deviation compared with the experimental data from the two groups [25, 26]. Hence the data from Grube [20] were not used in the present assessment.

Table 1. Summary of the experimental phase diagram and thermodynamic data in the Mg-Pb and Mg-Bi systems.

Systems	Type of experimental data	Experimental technique	Quoted mode ^a	Reference	
Mg-Pb	Liquidus from 0 to 100 at. % Pb	TA	□	[20]	
	Liquidus from 0 to 82 at. % Pb	TA	■	[21]	
	Liquidus and solidus from 0 to 20 at. % Pb, solid solubility Pb in (Mg)	TA, MA Resistivity	■	[22]	
	Liquidus and solidus from 0 to 20 at. % Pb, solid solubility Pb in (Mg)	TA, MA	■	[23]	
	Liquidus from 80 to 100 at. % Pb	TA	■	[24]	
	Liquidus from 0 to 100 at. % Pb, solid solubility Pb in (Mg) and solid solubility Mg in (Pb)	DTA	■	[25]	
	Liquidus from 20 to 100 at. % Pb	DTA	■	[26]	
	Liquidus and solidus from 80 to 100 at. % Pb	DTA	■	[27]	
	Solid solubility Pb in (Mg)	X-ray	■	[28]	
	Solid solubility Mg in (Pb)	HM	■	[29]	
	Enthalpy of mixing and activity of liquid		CA	■	[33]
			ISP	■	[32]
	Enthalpy of mixing of liquid	EMF	+	[30, 31]	
	Activity of Mg in liquid	EMF	■	[30, 31, 34-36]	
	Enthalpy increments of Mg ₂ Pb		EMF	■	[37]
			CA	■	[19, 33]
	Enthalpy of formation for Mg ₂ Pb		—	■	[38]
		CA	■	[33, 39, 40]	
Mg-Bi		—	■	[25]	
	Liquidus from 0 to 82 at. % Bi	TA	■	[41]	
	Liquidus from 0 to 100 at. % Bi	TA	■	[42]	
	Liquidus from 30 to 45 at. % Bi	TA	■	[43]	
	Solidus in Mg-rich region		TA	■	[42]
			RC	■	[44]
	Solid solubility Bi in (Mg)		RES	■	[41, 44]
			X-ray	■	[28]
	Gibbs energy of mixing and activity of Mg	VP	■	[45, 50]	
	Activity of Mg in liquid	EMF	■	[45, 46, 48, 50]	
Partial Gibbs energy of Mg	EMF	■	[46, 47, 49, 50]		
Enthalpy of formation for Mg ₃ Bi ₂		CA	■	[38, 51]	
		EMF	■	[49]	
	—	■	[52, 53]		

TA, thermal analysis; DTA, differential thermal analysis; MA, metallographic analysis; HM, hardness measurements; CA, calorimetry analysis; ISP, isopiestic technique; EMF, electromotive force; RC, Resistivity and conductivity; RES, resistometry; VP, vapor pressure

^a Indicates whether the data are used or not used in the parameter optimization: ■ used; □ not used but estimated to be reliable data for checking the modeling; + not used.

Vosskühler [22] and Raynor [23] determined the solidus of (Mg) by resistivity method and metallographic analysis. Graham et al. [27] determined the solidus of (Pb) by TA. Using metallography, X-ray diffraction (XRD) analysis and TA technique, the solubilities of Pb in (Mg) were determined by several groups [22, 23, 25, 28]. The solubilities of Mg in (Pb) were determined by Kurnakow et al. [29] and Dobovisek and Paulin [25]. These data showed a good agreement, and thus were included in the present optimization.

The enthalpy of mixing for liquid between 822K and 1223K were measured by several groups [30-33] using the mixing calorimetry technique, the isopiestic technique or electromotive force (emf) technique. However, the results from Lantratov [30] and Sryvalin et al. [31] indicated a large deviation from the data of Eldridge et al. [32] and Sommer et al. [33]. Consequently, these data [30, 31] were not used in the present optimization. The mixing enthalpies of liquid phase from Sommer et al. [33] indicates a temperature dependence, which manifested the existence of the short-range order behavior in the liquid phase. The activities of Mg in the liquid phase were measured by means of isopiestic technique [32] and emf technique [30, 31, 34-36]. These reported data agreed well with each other and were all considered in the present optimization.

The enthalpy increments of Mg₂Pb in the temperature range from 300 to 1400 K were measured by Cacciamani et al. [19], Sommer et al. [33] and Knappwost [37]. The enthalpy of formation for Mg₂Pb was measured by several groups [25, 33, 38-40]. These data were all included in this optimization.

2.2 The Mg-Bi system

Grube et al. [41, 42] are the pioneers for the experimental investigation on the Mg-Bi phase diagram. They determined this system over the whole composition range by means of TA. The liquidus in the composition range from 30 to 46 at. % Bi were elaborately measured again by Wobst [43] using the TA. The solubilities of Bi in (Mg) and the solidus of (Mg) were measured by Foote and Jette [28] and Vosskühler [44] using XRD analysis and resistometry, respectively. The reported experimental data showed a good agreement with each other, and were included in the optimization.

Thermodynamic properties of the Mg-Bi solution were measured by several groups [45-50]. Vetter and Kubaschewski [45] and Prasad et al. [50] determined the Gibbs energy of mixing of liquid, activities of Mg in liquid and partial Gibbs energy at 1123 K and 973 K by means of the vapor pressure method. Using the emf technique, Egan [46, 48] determined the activities of Mg at different temperatures. The partial Gibbs

energies of Mg were measured by Moser and Krohn [49], Heus and Egan [47] and Egan [46] by means of emf technique. Prasad et al. [50] extrapolated the experimental partial Gibbs energies of Mg [49] to a more wide composition range by using the Gibbs-Duhem function. The enthalpy of formation for Mg₃Bi₂ was determined by several groups [38, 49, 51-53]. All these data were considered in the present assessment.

Several groups of authors [4-8] determined the short-range order behavior of the liquid phase in the Mg-Bi system. According to the results for the enthalpy of mixing, Kawakami [4] found that the intermetallic compounds shared similar chemical bonding with their corresponding melting phase. Cohen and Sak [5] and Faber [6] thought that this might be due to the strong nonmetallic Mg-Bi bond. Ilchner and Wagner [7] found that the molten alloys of Mg-Bi showed a low value of conductivity and the value was almost 0 at the Mg₃Bi₂ composition according to the electrical conductivity measurements. The results confirmed the existences of the Mg-Bi bond and the bonds reached the maximum at the compound composition. Further Weber et al. [8] confirmed this standpoint by means of neutron diffraction and XRD. All these experimental results show that there exists a short-range order behavior in the liquid phase of the Mg-Bi system. The Mg-Bi system was also reviewed by Nayeb-Hashemi and Clark [54].

3. Thermodynamic model

3.1 Unary phase

The Gibbs energy functions of pure elements Mg, Pb and Bi are taken from the SGTE compilation by Dinsdale [55] and described by:

$$G_i(T) - H_i^{SER} = A + BT + CT \ln T + DT^2 + ET^{-1} + IT^7 + JT^{-9} \quad (1)$$

where H_i^{SER} is the molar enthalpy of the element i at 1 bar and 298.15 K in its standard element reference (SER) state, and T is the absolute temperature. The last two term in Eq.(4) are used only outside the ranges of stability, the term IT^7 for a liquid below the melting point and JT^{-9} for solid phases above the melting point.

3.2 Solid solution phases: Fcc_A1 and Hcp_A3

The solid solution phases are described by the substitutional solution model. The Gibbs energy is described by Redlich-Kister (R-K) polynomial [56]:

$$G_m^\Phi - H^{SER} = x_A^0 G_A^\Phi + x_B^0 G_B^\Phi + RT(x_A \ln x_A + x_B \ln x_B) + {}^{cs}G_m^\Phi \quad (2)$$

$${}^{ex}G_m^\Phi = x_A x_B \sum_{j=0}^n {}^jL_{A,B}^\Phi (x_A - x_B)^j \quad (3)$$

where A is Mg, B is Pb or Bi. Φ represents the Fcc_A1 and Hcp_A3. ${}^0G_i^\Phi$ ($i=A$ or B) is the molar Gibbs energy of the pure element. ${}^{ex}G_m^\Phi$ is the excess Gibbs energy. ${}^jL_{A,B}^\Phi$ is the j^{th} interaction parameter for the solution phase Φ . It is expressed as:

$${}^jL_{A,B}^\Phi = a_j + b_j T \quad (4)$$

where a_j and b_j are variables to be evaluated from the experimental data.

3.3 The liquid phase

Due to the short-range order behavior of the liquid phase in both Mg-Pb and Mg-Bi systems, the associate model is used to describe the liquid phase for these two systems. Meanwhile, the substitutional solution model is also used for the sake of model compatibility to the multi-component Mg alloy thermodynamic database [17].

The molar Gibbs energy of substitutional solution model for liquid phase is described with the analogous equations (Eqs. 2 and 3). In the associate model, the liquid phase is assumed to contain three species, (Mg, Mg₂Pb, Pb) for the Mg-Pb system and (Bi, Mg₃Bi₂, Mg) for the Mg-Bi system. The molar Gibbs energy of the liquid for the Mg-Pb system and the Mg-Bi system is written as:

$$G_m^L - H^{SER} = y_{Mg} {}^0G_{Mg}^L + y_B {}^0G_B^L + y_{Mg_mPb_n} {}^0G_{Mg_mPb_n}^L + RT(y_{Mg} \ln y_{Mg} + y_B \ln y_B + y_{Mg_mPb_n} \ln y_{Mg_mPb_n}) + {}^{ex}G_m^L \quad (5)$$

where y_i is the mole fractions of each species in the liquid phase and B represents Pb or Bi. ${}^0G_{Mg_mPb_n}^L$ is the hypothetical formation Gibbs energy for the compound Mg₂Pb and Mg₃Bi₂ in the liquid phase, which is described in Eq. 6. The coefficients a and b are to be evaluated in the present work. ${}^{ex}G_m^L$ is the excess Gibbs energy, expressed in Eq.7.

$${}^0G_{Mg_mPb_n}^L = m {}^0G_{Mg}^L + n {}^0G_B^L + a + bT \quad (6)$$

$$\begin{aligned} {}^{ex}G_m^L = & y_{Mg} y_B \sum_{j=0}^{\infty} {}^jL_{Mg,B}^L (y_{Mg} - y_B)^j + \\ & + y_{Mg} y_{Mg_mPb_n} \sum_{j=0}^{\infty} {}^jL_{Mg,Mg_mPb_n}^L (y_{Mg} - y_{Mg_mPb_n})^j \\ & + y_{Mg_mPb_n} y_B \sum_{j=0}^{\infty} {}^jL_{Mg_mPb_n,B}^L (y_{Mg_mPb_n} - y_B)^j \end{aligned} \quad (7)$$

where ${}^jL_{Mg,B}^L$, ${}^jL_{Mg,Mg_mPb_n}^L$, ${}^jL_{Mg_mPb_n,B}^L$ is the j^{th} interaction parameter of the liquid phase.

3.4 Intermetallic phases

The Mg₂Pb phase is modeled as stoichiometric phase in view of the negligible homogeneities. Since the experimental data on the enthalpy increments of Mg₂Pb in a wide temperature range are available [19, 33, 37], it is preferable to express its Gibbs energy relative to the SER state. The Gibbs energy of Mg₂Pb is given by the following expression:

$$G_m^{Mg_2Pb} - \frac{2}{3} H_{Mg}^{SER} - \frac{1}{3} H_{Pb}^{SER} = a + bT + cT \ln T + dT^2 + eT^{-1} \quad (8)$$

where a , c , d , e is relative to the enthalpy increments and the formation enthalpy of Mg₂Pb.

The Mg₃Bi₂ phase has two forms: α phase (low temperature form, La₂O₃ proto-type, P3m1space group) [57] and β phase (high temperature form, Ag₂S proto-type, Im $\bar{3}$ m space group) [58]. According to the reported experimental data [42], both α -Mg₃Bi₂ and β -Mg₃Bi₂ have a narrow homogeneity range. Therefore, in the present work they are both described using the sublattice model (Bi, Va)_{0.4}Mg_{0.6}. The Gibbs energy of Mg₃Bi₂ phases can be expressed as:

$$\begin{aligned} G_m^{Mg_3Bi_2} - H^{SER} = & y_{Bi} {}^0G_{Bi:Mg}^{Mg_3Bi_2} + y_{Va} {}^0G_{Va:Mg}^{Mg_3Bi_2} + \\ & + 0.4RT(y_{Bi} \ln y_{Bi} + y_{Va} \ln y_{Va}) \\ & + y_{Bi} y_{Va} \sum_{j=0}^n {}^jL_{Bi,Va}^{Mg_3Bi_2} (y_{Bi} - y_{Va})^j \end{aligned} \quad (9)$$

where y_{Bi} and y_{Va} are the site fractions of Bi and Va in the first sublattice, respectively. ${}^jL_{Bi,Va}^{Mg_3Bi_2}$ is the interaction parameters between Bi and vacancy. ${}^0G_{Bi:Mg}^{Mg_3Bi_2}$ and ${}^0G_{Va:Mg}^{Mg_3Bi_2}$ are the Gibbs energy of formation of the end-members. They are given by the following equations:

$${}^0G_{Bi:Mg}^{Mg_3Bi_2} = 2 {}^0G_{Bi}^{rho_A7} + 3 {}^0G_{Mg}^{hcp_A3} + A + BT \quad (10-a)$$

$${}^0G_{Va:Mg}^{Mg_3Bi_2} = 3 {}^0G_{Mg}^{hcp_A3} + A_0 + B_0 T \quad (10-b)$$

A , B , A_0 , B_0 are the parameters to be optimized.

Table 2. Summary of the thermodynamic parameters in the Mg-Pb and Mg-Bi systems

Phases	Set 1	Set 2
Mg-Pb system		
Liquid:	(Mg, Pb) ₁	(Mg, Mg ₂ Pb, Pb) ₁
	${}^0L_{Mg,Pb}^{Liquid} = -32873.29 + 4.45T$	${}^0G_{Mg_2Pb}^{Liquid} - 2G_{Mg}^{Liquid} - G_{Pb}^{Liquid}$

Table continued on next page

	${}^1L_{Mg,Pb}^{Liquid} = -19584.57 + 11.45T$	$= -36618.56 + 3.17T$
		${}^0L_{Mg,Pb}^{Liquid} = -16698.13 - 5.43T$
		${}^0L_{Mg,Mg_2Pb}^{Liquid} = -2227.86 + 0.237T$
		${}^0L_{Mg_2Pb,Pb}^{Liquid} = -8462.74$
Hcp_A3:	(Mg, Pb) ₁ Va _{0.5}	
	${}^0L_{Mg,Pb:Va}^{Hcp_A3} = -4679.16 - 20.33T$	${}^0L_{Mg,Pb:Va}^{Hcp_A3} = -8732.20 - 15.72T$
	${}^1L_{Mg,Pb:Va}^{Hcp_A3} = -9549.62$	${}^1L_{Mg,Pb:Va}^{Hcp_A3} = -11593.00$
Fcc_A1:	(Mg, Pb) ₁ Va ₁	
	${}^0L_{Mg,Pb:Va}^{Fcc_A1} = -10419.65 - 3.28T$	${}^0L_{Mg,Pb:Va}^{Fcc_A1} = -13651.98 + 0.737T$
Mg ₂ Pb:	Mg _{0.66667} Pb _{0.33333}	
	${}^0G_{Mg_2Pb}^{Mg_2Pb} - \frac{2}{3}H_{Mg}^{SER} - \frac{1}{3}H_{Pb}^{SER} =$	${}^0G_{Mg_2Pb}^{Mg_2Pb} - \frac{2}{3}H_{Mg}^{SER} - \frac{1}{3}H_{Pb}^{SER} =$
	$-21874.47 + 23.26T - 7.38T \ln T$	$-23514.15 + 64.83T - 14.20T \ln T$
	$-0.018068T^2 + 27327.4028T^{-1}$	$-0.01275T^2 + 37683.32T^{-1}$
Mg-Bi system		
Liquid:	(Bi, Mg) ₁	(Bi, Mg ₃ Bi ₂ , Mg) ₁
	${}^0L_{Bi,Mg}^{Liquid} = -39124.75 - 29.383T$	${}^0G_{Mg_3Bi_2}^{Liquid} - 3G_{Mg}^{Liquid} - 2G_{Bi}^{Liquid}$
	${}^1L_{Bi,Mg}^{Liquid} = -6880.83 + 13.226T$	$= -144293.32 + 10.49T$
	${}^2L_{Bi,Mg}^{Liquid} = 12285.53 + 10.237T$	${}^0L_{Bi,Mg}^{Liquid} = -45804.176 - 12.83T$
		${}^1L_{Bi,Mg}^{Liquid} = 6250.69$
		${}^0L_{Mg_3Bi_2,Bi}^{Liquid} = 14050.46 - 34.81T$
Hcp_A3:	(Bi, Mg) ₁ Va _{0.5}	
	${}^0L_{Bi,Mg:Va}^{Hcp_A3} = -36583.24 - 2.47T$	${}^0L_{Bi,Mg:Va}^{Hcp_A3} = -35913.51 - 18.44T$
α -Mg ₃ Bi ₂ :	Mg _{0.6} (Bi, Va) _{0.4}	
	${}^0G_{Mg:Bi}^{\alpha-Mg_3Bi_2} - 0.6{}^0G_{Mg}^{Hcp_A3} - 0.4{}^0G_{Bi}^{Rho_A7}$	${}^0G_{Mg:Bi}^{\alpha-Mg_3Bi_2} - 0.6{}^0G_{Mg}^{Hcp_A3} - 0.4{}^0G_{Bi}^{Rho_A7}$
	$= -34976.85 + 9.481T$	$= -33728.77 + 2.063T$
	${}^0G_{Mg:Va}^{\alpha-Mg_3Bi_2} - 0.6{}^0G_{Mg}^{Hcp_A3}$	${}^0G_{Mg:Va}^{\alpha-Mg_3Bi_2} - 0.6{}^0G_{Mg}^{Hcp_A3}$
	$= 11023.56 + 9.365T$	$= 13957.31 + 2.12T$
	${}^0L_{Mg:Bi:Va}^{\alpha-Mg_3Bi_2} = -18050.09 - 6.40T$	${}^0L_{Mg:Bi:Va}^{\alpha-Mg_3Bi_2} = -21286.10 + 1.201T$
	${}^1L_{Mg:Bi:Va}^{\alpha-Mg_3Bi_2} = 11884.32$	${}^1L_{Mg:Bi:Va}^{\alpha-Mg_3Bi_2} = 12078.81$

Table continued on next page

$$\begin{array}{l}
 \beta\text{-Mg}_3\text{Bi}_2: \quad \text{Mg}_{0.6}(\text{Bi}, \text{Va})_{0.4} \\
 {}^0G_{\text{Mg:Bi}}^{\beta\text{-Mg}_3\text{Bi}_2} - 0.6 {}^0G_{\text{Mg}}^{\text{Hcp_A3}} - 0.4 {}^0G_{\text{Bi}}^{\text{Rho_A7}} \quad {}^0G_{\text{Mg:Bi}}^{\beta\text{-Mg}_3\text{Bi}_2} - 0.6 {}^0G_{\text{Mg}}^{\text{Hcp_A3}} - 0.4 {}^0G_{\text{Bi}}^{\text{Rho_A7}} \\
 = -2443.72 - 24.09T \quad \quad \quad = -23007.54 - 8.973T \\
 {}^0G_{\text{Mg:Va}}^{\beta\text{-Mg}_3\text{Bi}_2} - 0.6 {}^0G_{\text{Mg}}^{\text{Hcp_A3}} \quad {}^0G_{\text{Mg:Va}}^{\beta\text{-Mg}_3\text{Bi}_2} - 0.6 {}^0G_{\text{Mg}}^{\text{Hcp_A3}} \\
 = -6718.51 + 25.66T \quad \quad \quad = -1769.10 + 29.7T \\
 {}^0L_{\text{Mg:Bi,Va}}^{\beta\text{-Mg}_3\text{Bi}_2} = -18403.45 \quad {}^0L_{\text{Mg:Bi,Va}}^{\beta\text{-Mg}_3\text{Bi}_2} = -19966.69 - 3.02T
 \end{array}$$

Set 1 indicated the substitutional solution model and Set 2 indicated the associate mode

4. Results and discussion

The assessment was carried out by using the PARRAOT module of Thermo-Calc [59] which works by minimizing the square sum of the errors. The step-by-step optimization procedure [60] was utilized in the present assessment. In the optimization, each piece of experimental information was given a certain weight based on uncertainties of the data. The present work is a continuing effort of our previous attempts [61-62] to establish a thermodynamic database for multicomponent Al alloys.

The optimization starts with the thermodynamic properties for the liquid phase, including the activities and mixing enthalpies. Then, the parameters for the solid solution phases (Mg-hcp, Pb-fcc) were optimized by using the experimental solubilities data [22, 23, 25, 28, 29, 41, 44]. Next, the parameters for the Mg₂Pb and Mg₃Bi₂ phases were evaluated by using the enthalpy increments [19, 33, 37], the formation enthalpy [8, 25, 33, 38-40, 49, 51, 52] and the phase diagram data [42].

Finally, all the parameters were optimized simultaneously based on the experimental data to get two sets of self-consistent thermodynamic parameters. The finally obtained parameters for the Mg-Pb and Mg-Bi binary systems are listed in Table 2. The calculated invariant equilibria in the Mg-Pb and Mg-Bi systems along with the experimental data are summarized in Table 3.

4.1 The Mg-Pb system

Figure 1 shows the calculated Mg-Pb phase diagrams using both the substitutional solution model and the associate model for the liquid phase. It can be seen that the calculated phase diagram can reproduce well the experimental data [20-29]. The calculated compositions and temperatures for the invariant reactions in Table 3 show that the calculation using the associate model can agree more reasonable with the measured data than that using the substitutional solution model. During the assessment using the substitutional solution model, the attempt to use more parameters resulted in little improvement in the

calculated compositions. It indicates that the associate model is more reasonable to handle this system than the substitutional model.

Table 3. Calculated invariant equilibria in the Mg-Pb and Mg-Bi systems compared with experimental data

Systems	Reaction	Compositions			T/K	Reference
Mg-Pb system		at.% Pb				
	Liquid=Mg ₂ Pb	33.33	33.33		822.65±1	[39]
		35	35		822.15±0.3	[26]
		33.33	33.33		823.15±3	[25]
		33.33	33.33		823.15	[37]
		33.33	33.33		823.15	[21]
		33.33	33.33		824.1	This work (Set 1)
		33.33	33.33		823.4	This work (Set 2)
	Liquid=Mg ₂ Pb+(Mg)	19.1	33.33	7.75	739.35	[26]
		—	33.33	7.8	739.15±1	[25]
		—	33.33	7.14	739.15	[28]
		19.1	33.33	9.75	738.15	[23]
		19.1	33.33	9.1	739.15	[22]
		20	33.33	—	748.15	[21]
		19.2	33.33	—	732.15	[20]
		16.51	33.33	8.71	732	This work (Set 1)
	19.29	33.33	7.41	737.05	This work (Set 2)	
	Liquid=Mg ₂ Pb+(Pb)	83.5	33.33	94.7	521.15±1	[27]
		83	33.33	—	521.85	[26]
		—	33.33	94.1	525.15±2	[25]
		84.3	33.33	100	526.15	[21]
79.15		33.33	100	520.15	[20]	
80.7		33.33	94.66	517.29	This work (Set 1)	
82.65		33.33	94.63	520.22	This work (Set 2)	

Table continued on next page

		at.% Bi				
Mg-Bi system	Liquid= β -Mg ₃ Bi ₂	40	40		988.15	[41]
		40	40		1096.15	[42]
		40	40		1094.15	[43]
		40	40		1090.15	This work (Set 1)
		40	40		1093.82	This work (Set 2)
	Liquid= α -Mg ₃ Bi ₂ + (Mg)	17.76	40	0	825.15	[41]
		14.3	35	1.5	825.15±2	[42]
		—	—	—	826.15	[43]
		11.63	36.45	1.17	830.76	This work (Set 1)
		12.83	34.54	1.06	823.28	This work (Set 2)
	Liquid= α -Mg ₃ Bi ₂ +Bi	~100	40	~100	541.15	[41]
		95.7	40	~100	533.15±2	[42]
		95.87	40	100	537.38	This work (Set 1)
		95.8	40	100	532.87	This work (Set 2)
	β -Mg ₃ Bi ₂ = α -Mg ₃ Bi ₂ +Liquid	38.7	39.3	31.5	959.15	[42]
		38.7	~39.3	31.5	961.15	[43]
		37.72	39.47	31.13	957.3	This work (Set 1)
		38.81	39.07	32.05	961.64	This work (Set 2)
	β -Mg ₃ Bi ₂ = α -Mg ₃ Bi ₂	40	40		973.15	[42]
		40	40		976.15	[43]
40		40		967.05	This work (Set 1)	
40		40		971.37	This work (Set 2)	

Figure 2 presents the calculated enthalpies of mixing for liquid at 822, 943, 1033 and 1223 K along with the experimental data [32, 33]. The calculated activity of Mg in the liquid phase at 923 K compared with the experimental data [30-32, 34-36] is shown in Figure 3. From the two figures, we can see that the calculated values using the associate model agree better with the experimental data than those using the substitutional solution model. Figure 4 presents the comparison between the calculated enthalpy of formation of Mg₂Pb using the two models at 298.15 K and the experimental data available in the literature [25, 33, 38-40]. The calculated values using the two models are almost the same (-17.88 kJ/mol-atoms for the substitutional solution model and -17.89 kJ/mol-

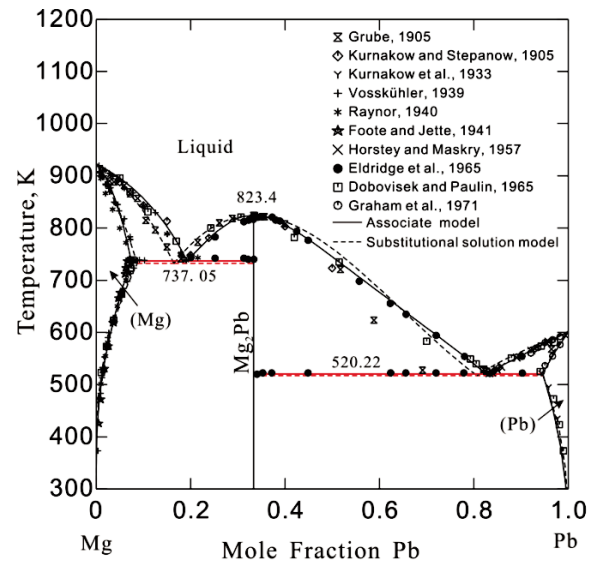


Figure 1. Calculated Mg-Pb phase diagram using both the substitutional solution model (dashed line) and the associate model (solid line) along with experimental data [20-29].

atoms for the associate model) and they can both reasonably reproduce the available experimental data. The calculated heat of fusion for the Mg₂Pb phase is 15.22 kJ/mol-atoms with the associate model closer than 16.69 kJ/mol-atoms with the substitutional solution model to the data reported by Eldridge et al. [32] (14.33 kJ/mol-atoms) and Sommer et al. [33]

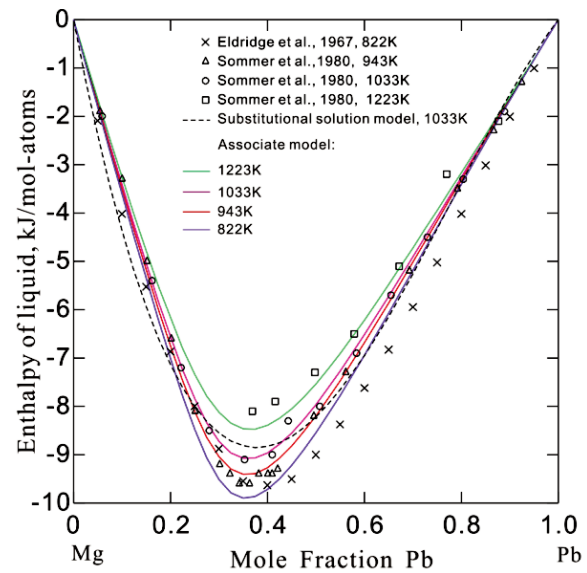


Figure 2. Calculated enthalpies of mixing of the Mg-Pb system for liquid at 822, 943, 1033 and 1223 K using both the substitutional solution model (dashed line) and the associate model (solid line) with the experimental data [32, 33]. The reference states are liquid Mg and liquid Pb.

(13.4 kJ/mol-atoms). In Figure 5, the calculated enthalpy increment for the compound Mg_2Pb is compared with the experimental data [19, 33, 37]. It again indicates that the description with the associate model is better than that with the substitutional solution model, especially in the liquid region.

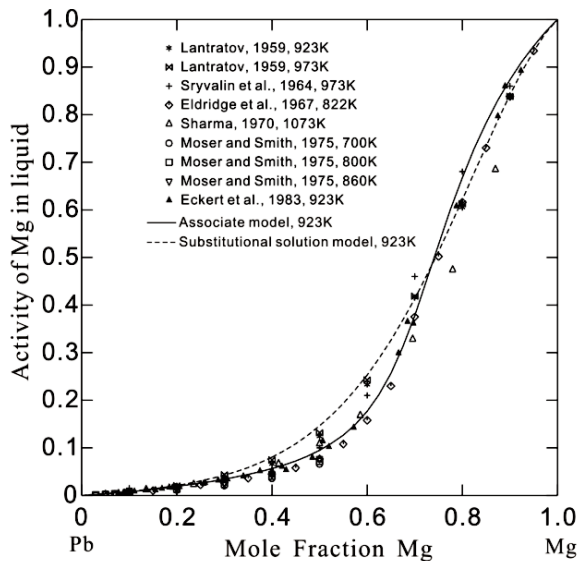


Figure 3. Calculated activity of Mg in liquid at 923 K for the Mg-Pb system using both the substitutional solution (dashed line) model and the associate model (solid line) with the experimental data [30-32, 34-36]. The reference state is liquid Mg.

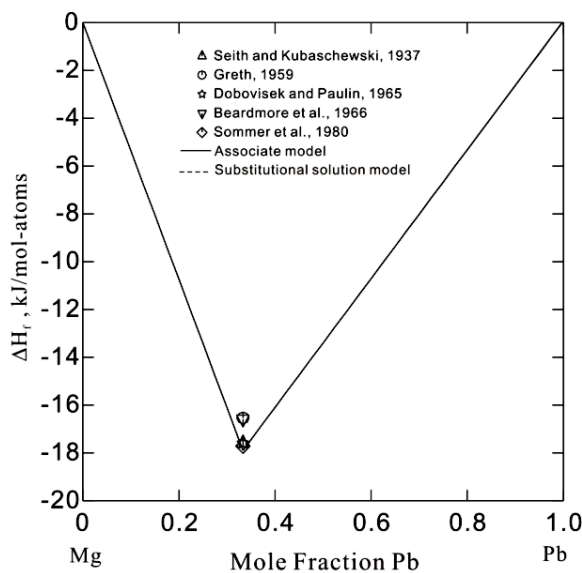


Figure 4. Calculated enthalpies of formation at 298.15 K for the Mg-Pb system using both the substitutional solution model and the associate model, compared with the experimental data [25, 33, 38-40]. The reference states are Hcp Mg and Fcc Pb.

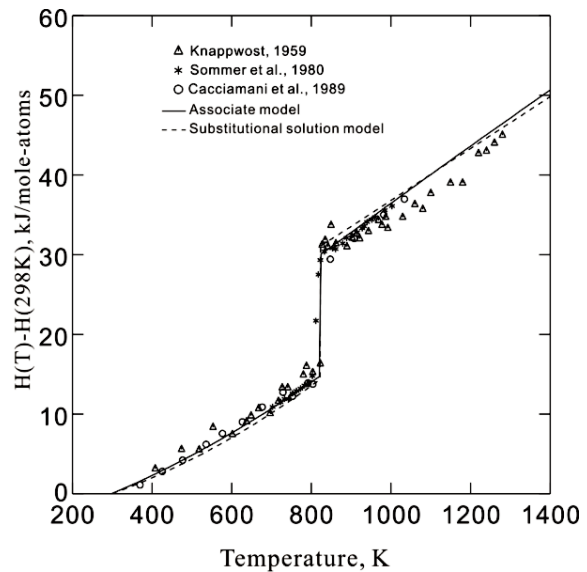


Figure 5. Calculated $H(T)-H(298K)$ for Mg_2Pb phase using both the substitutional solution model (dashed line) and the associate model (solid line) with the experimental data [19, 33, 37].

4.2 The Mg-Bi system

Table 4 lists the comparison of parameters between this work and Niu et al. [13]. Less parameters of the liquid phase in both models are used in the present work. Moreover, the term $cT \ln T$ for the α - Mg_3Bi_2 in the previous assessment [10, 13] is not utilized in the present work.

The calculated Mg-Bi phase diagrams using the substitutional solution model and the associate model along with the experimental data [28, 41-44] are shown in Fig.6.

Table 4. Parameters number of this work and Niu et al. [13] in the Mg-Bi system

	This work		Niu et al. [13] with the associate model
	substitutional model	associate model	
Liquid	6	7	11
Hcp_A3	2	2	2
α - Mg_3Bi_2 :	7	4	11
β - Mg_3Bi_2	5	6	7

As can be seen from Figure 6, the phase diagram using the substitutional solution model can reproduce the experimental data well from 0 to 45 at.% Bi, but not well in the Bi-rich side though the parameters for the liquid phase approach to the 3rd order. However, the associate model can reproduce all the experimental data [28, 41-44] excellently over the whole composition range. Similarly, the calculated compositions and temperatures for the invariant

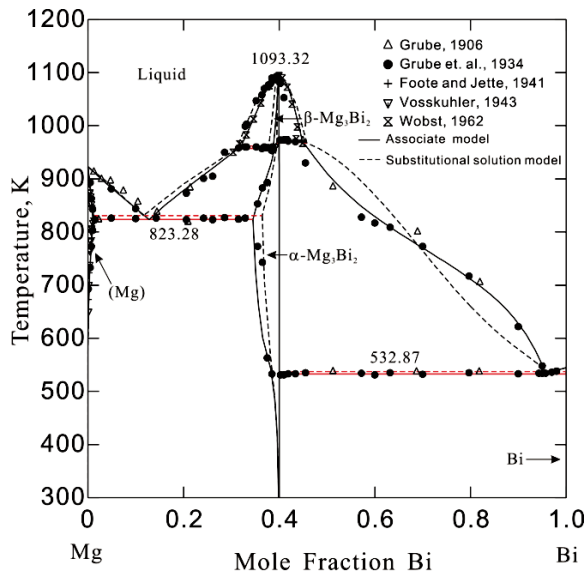


Figure 6. Calculated Mg-Bi phase diagram using both the substitutional solution model (dashed line) and the associate model (solid line) along with experimental data [28, 41-44].

reactions listed in Table 3 show that the calculation with the associate model agrees more reasonable with the measured data than that with the substitutional solution model. It indicates that the associate model has advantages to describe such liquidus.

Figure 7 shows the calculated activities of Mg in the liquid phase with the experimental data [45, 46,

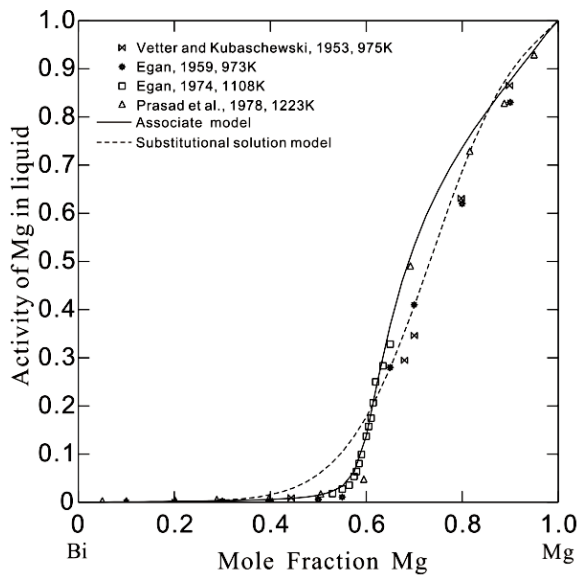


Figure 7. Calculated activity of Mg in liquid at 1108 K for the Mg-Bi system using both the substitutional solution (dashed line) model and the associate model (solid line) with the experimental data [45, 46, 48, 50]. The reference state is liquid Mg.

48, 50] at 1108 K. The experimental data from 40 to 60 at.% Mg could not be described well by the substitutional solution model. However, the associate model could reproduce the experimental data reasonably over the whole composition range. Figure 8 shows the calculated partial Gibbs energy of Mg in the liquid phase with the literature data [47-50] at 1123 K. Both the associate model and substitutional solution models could reproduce well with the reported experimental data. Figure 9 presents the calculated Gibbs energy of mixing for the liquid phase at 1123 K compared with the experimental data [45, 50]. It can be seen that a better agreement between the calculated results and experimental data lies in the associate model than the substitutional solution model. Figure 10 shows the comparison between the calculated enthalpy of formation for the Mg_3Bi_2 phase at 298.15 K using both substitutional solution and associate models along with the experimental data [8, 38, 49, 51, 52]. Similar results were obtained using both the models.

Figures 11 and 12 illustrate the fractions of the species in the liquid phase with the function of composition at different temperatures for the Mg-Pb and Mg-Bi systems which show the short-range order behavior in the liquid phase. The highest site fractions of Mg_2Pb and Mg_3Bi_2 species are around the composition of 33 at.% Pb and 40 at.% Bi which is reasonable for describing the experimental phenomena. With the increasing temperature, as

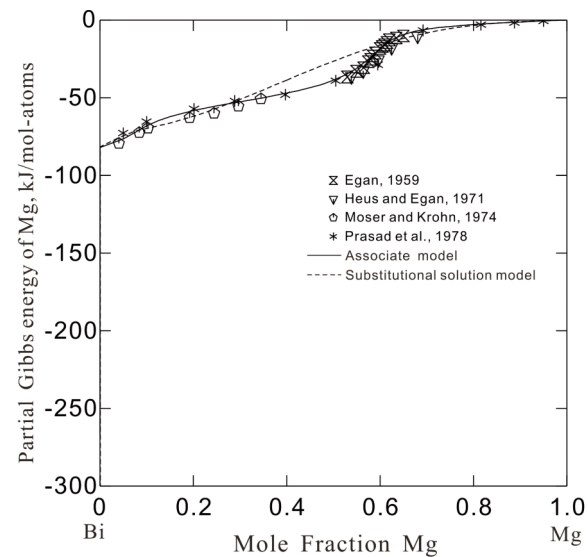


Figure 8. Calculated partial Gibbs energy of Mg in liquid at 1123 K for the Mg-Bi system using both the substitutional solution model (dashed line) and the associate model (solid line) with the experimental data [47-50]. The reference states are liquid Mg and liquid Bi. The experimental data [49] were extrapolated by Prasad [50] according to the experimental data.

expected, the site fractions of Mg_2Pb and Mg_3Bi_2 species are decreasing due to the decomposition of chemical bond.

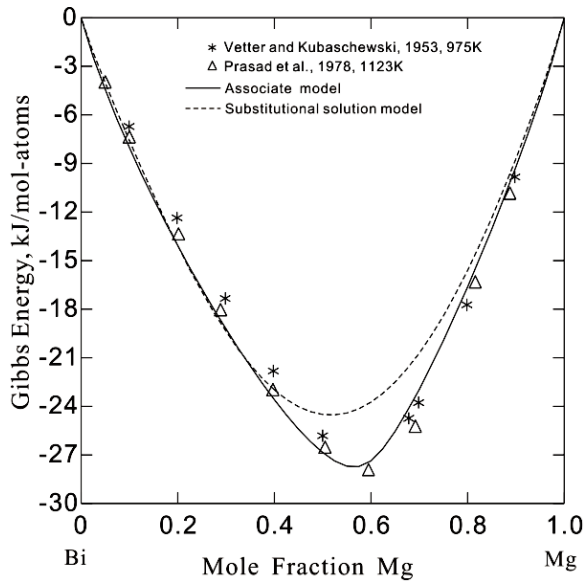


Figure 9. Calculated Gibbs energy of mixing of the Mg-Bi system at 975 K using both the substitutional solution model (dashed line) and the associate model (solid line) with the experimental data [45, 50]. The reference states are liquid Mg and liquid Bi. And

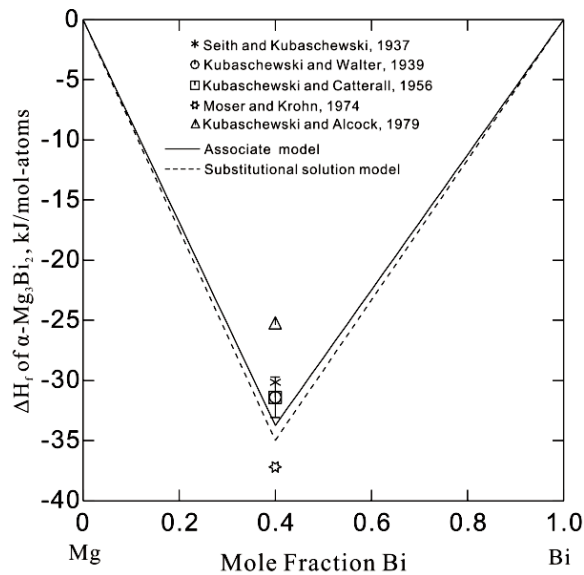


Figure 10. Calculated enthalpies of formation at 298.15 K for the Mg-Bi system using both the substitutional solution model (dashed line) and the associate model (solid line), compared with the experimental data [38, 49, 51-53]. The reference states are Hcp Mg and Rho Bi.

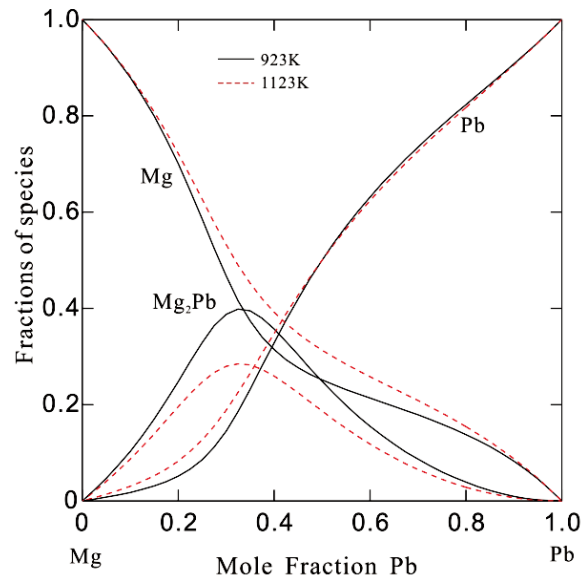


Figure 11. Fractions of the species in the liquid phase of the Mg-Pb system at 923 and 1123 K

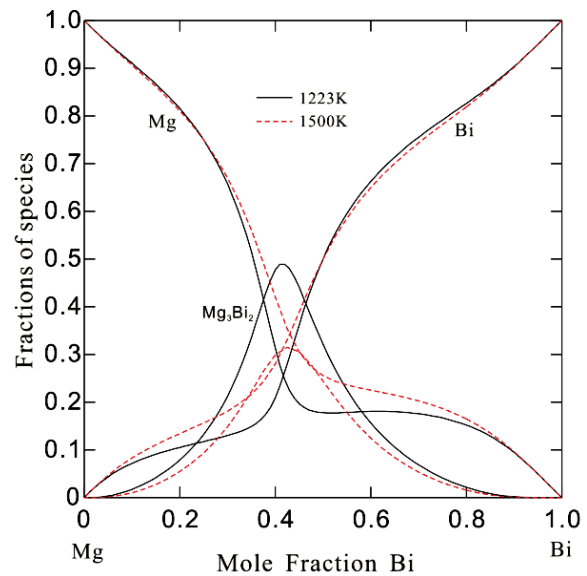


Figure 12. Fractions of the species in the liquid phase of the Mg-Bi system at 1223 and 1500 K.

5. Summary

A critical assessment was carried out for the experimental phase diagram and thermodynamic data in the Mg-Pb and Mg-Bi systems.

The Mg-Pb and Mg-Bi systems were modeled by means of the CALPHAD approach. The substitutional model and associate model were used to describe the liquid phase in the Mg-Pb and Mg-Bi systems.

For the binary system with the nonsymmetrical

liquidus and the short-range order behavior in the liquid phase, an associated model can describe the phase transitions more accurately than the substitutional solution model.

Acknowledgements

The financial support from the National Science Foundation for Youth of China (Grant No. 51101172), the National Basic Research Program of China (Grant No. 2011CB610401) and the Sino-German cooperation group "Microstructure in Al alloys" (Grant No. GZ755) is greatly acknowledged.

References

- [1] B.L. Mordike, T. Ebert, Mater. Sci. Eng. A, 302 (2001) 37-45.
- [2] V. Goryany and P.J. Mauk, J. Min. Metall. Sect. B., 43 B (2007) 85-97.
- [3] Y.-X. Wang, J.-X. Zhou, J. Wang, T.-J. Luo, Y.-S. Yang, T. Nonferr. Metal. Soc., 21 (2011) 711-716.
- [4] M. Kawakami, Sci. Rep. Tohoku Imp. Univ., 19 (1930) 521-549.
- [5] M.H. Cohen, J. Sak, J. Non-Cryst. Solids, 8-10 (1972) 696-701.
- [6] T.E. Faber, Introduction to the Theory of Liquid Metals, University Press, Cambridge, 1972, p.1.
- [7] B.R. Ilschner, C. Wagner, Acta Metall., 6 (1958) 712-713.
- [8] M. Weber, S. Steeb, P. Lamparter, Z. Naturforsch., 34a (1979) 1398-1403.
- [9] F. Sommer, Z. Metallkd., 73 (1982) 77-86.
- [10] O. Chang-Seok, K. Soo-Young, N.L. Dong, CALPHAD, 16 (1992) 181-191.
- [11] D. Nassyro, I.-H. Jung, CALPHAD, 33 (2009) 521-529.
- [12] M. Paliwal, I.-H. Jung, CALPHAD, 33 (2009) 744-754.
- [13] C. Niu, C. Li, Z. Du, C. Guo, Y. Jing, Acta Metall. Sin. (Engl. Lett.), 25 (2012) 19-28.
- [14] F. Sommer, Mater. Res. Soc. Symp. Proc., 19 (1983) 163-173.
- [15] R. Schmid, Y.A. Chang, CALPHAD, 9 (1985) 363-382.
- [16] A.D. Pelton, S.A. Degterov, G. Eriksson, C. Robelin, Y. Dessureault, Metall. Mater. Trans. B, 31B (2000) 651-659.
- [17] Y. Du, P.S. Wang, S.H. Liu, CALPHAD, 35 (2011) 523-532.
- [18] A.A. Nayeb-Hashemi, J.B. Clark, Bull. Alloy Phase Diagrams, 6 (1985) 56-66, 97-58.
- [19] G. Cacciamani, G. Borzone, A. Saccone, R. Ferro, J. Less-Common Met., 154 (1989) 109-113.
- [20] G. Grube, Z. Anorg. Chem., 44 (1905) 117-130.
- [21] N.S. Kurnakow, N.J. Stepanow, Z. Anorg. Chem., 46 (1905) 177-192.
- [22] H. Vosskühler, Z. Metallkd., 31 (1939) 109-111.
- [23] G.V. Raynor, J. Inst. Met., 66 (1940) 403-426.
- [24] G.W. Horsley, J.T. Maskry, J. Inst. Met., 86 (1957) 446-448.
- [25] B. Dobovisek, A. Paulin, Rud.-Metal. Zb., 3-4 (1965) 373-387.
- [26] J.M. Eldridge, E. Miller, K.L. Komarek, Trans. AIME, 233 (1965) 1304-1308.
- [27] J. C.D. Graham, J.A. Burgo, J.W. Cooper, C.L. Douglas, P.S. Gilman, W.T. Kelly, A. Nagelberg, 2 (1971) 2964-2965.
- [28] F. Foote, R. Jette, Trans. AIME, 143 (1941) 124-131.
- [29] N.S. Kurnakow, S.A. Pogodin, T.A. Vidusova, Izv. Inst. Fiz.-Khim. Anal., 6 (1933) 266-267.
- [30] M.F. Lantratov, Russ. J. Inorg. Chem., 4 (1959) 1415-1419.
- [31] I.T. Sryvalin, O.A. Esin, B.M. LePinskikh, Russ. J. Phys. Chem., 38 (1964) 1166-1172.
- [32] J.M. Eldridge, E. Miller, K.L. Komarek, Trans. AIME, 239 (1967) 570-572.
- [33] F. Sommer, J.J. Lee, B. Predel, Z. Metallkd., 71 (1980) 818-821.
- [34] R.A. Sharma, J. Chem. Thermodyn., 2 (1970) 373-389
- [35] Z. Moser, J.F. Smith, Metall. Trans., 6B, (1975) 653-659.
- [36] C.A. Eckert, R.B. Irwin, J.S. Smith, Metall. Trans., 14B (1983) 451-458.
- [37] A. Knappwost, Z. Phys. Chem., 21 (1959) 358-375.
- [38] W. Seith, O. Kubaschewski, Z. Electrochem., 43 (1937) 743-749.
- [39] H.J. Grethe, Calorimetry and Thermodynamics of Mg-Pb Alloys (quoted in [14]), thesis, Clausthal, 1959.
- [40] P. Beardmore, B.W. Howlett, B.D. Lichter, M.B. Bever, Trans. AIME, 236 (1966) 102-108.
- [41] G. Grube, Z. Anorg. Chem., 49 (1906) 83-87.
- [42] G. Grube, L. Mohr, R. Bornhak, Z. Elektrochem., 40 (1934) 143-150.
- [43] M. Wobst, Z. Phys. Chem., 219 (1962) 239-265.
- [44] H. Vosskühler, Metallwirtschaft, 22 (1943) 545-547.
- [45] F.A. Vetter, O. Kubaschewski, Z. Elektrochem., 57 (1953) 243-248.
- [46] J.J. Egan, Acta Metall., 7 (1959) 560-564.
- [47] R.J. Heus, J.J. Egan, Z. Phys. Chem., 74 (1971) 108-114.
- [48] J.J. Egan, J. Nucl. Mater., 51 (1974) 30-35.
- [49] Z. Moser, C. Krohn, Metall. Trans., 5 (1974) 979-985.
- [50] R. Prasad, V. Venugopal, P.N. Iyer, D.D. Sood, J. Chem. Thermodyn., 10 (1978) 135-141.
- [51] O. Kubaschewski, A. Walter, Z. Elektrochem., 45 (1939) 732-740.
- [52] O. Kubaschewski, J.A. Catterall, Thermodynamical Data of Alloys, Pergamon Press, London, 1956, p. 23.
- [53] O. Kubaschewski, C.B. Alcock, Metallurgwal Thermochemistry, 5th ed., Pergamon Press, New York, 1979, p. 30.
- [54] A.A. Nayeb-Hashemi, J.B. Clark, Bull. of Alloy Phase Diagrams, 6 (1985) 528-533.
- [55] A.T. Dinsdale, SGTE data for pure elements, CALPHAD, 15 (1991) 317-425.
- [56] O. Redlich, A.T. Kister, J. Ind. Eng. Chem. (Washington, D. C.), 40 (1948) 84,85-88.
- [57] E. Zintl, E. Husemann, Z. Phys. Chem., B21 (1933)

- 138-155.
- [58] A.C. Barnes, C. Guo, W.S. Howells, *J. Phys.: Condens. Matter*, 6 (1994) 467-471.
- [59] B. Sundman, B. Jansson, J.-O. Andersson, The Thermo-Calc databank system, *CALPHAD*, 9 (1985) 153-190.
- [60] Y. Du, R. Schmid-Fetzer, *J. Phase Equilib.*, 17 (1996) 311-324.
- [61] C. Tang, P. Zhou, D.D. Zhao, X. M. Yuan, Y. Tang, P. S. Wang, B. Hu, Y. Du, H.H. Xu, *J. Min. Metall. Sect. B-Metall.*, 48 (1) B (2012) 123 - 130.
- [62] Y. Wang, B. Hu, S. Liu, Y. Du, *J. Min. Metall. Sect. B-Metall.*, 49 (1) B (2013) 391 - 394.